Civil Engineering and Architecture 11(3): 1523-1537, 2023
DOI: 10.13189/cea.2023.110333 http://www.hrpub.org

Tuned Mass Damper Parameters Design by Means of Meta-Heuristic Optimization Algorithms

Abdelmajeed Alkasassbeh*, Bilal Yasin, Hatem Almasaeid

Department of Civil Engineering, Faculty of Engineering, Al al-Bayt University, 25113 Mafraq, Jordan

Received October 7, 2022; Revised January 30, 2023; Accepted February 23, 2023

Cite This Paper in the Following Citation Styles

***(a):** [1] Abdelmajeed Alkasassbeh, Bilal Yasin, Hatem Almasaeid , "Tuned Mass Damper Parameters Design by Means of Meta-Heuristic Optimization Algorithms," Civil Engineering and Architecture, Vol. 11, No. 3, pp. 1523 - 1537, 2023. DOI: 10.13189/cea.2023.110333.*

***(b):** Abdelmajeed Alkasassbeh, Bilal Yasin, Hatem Almasaeid (2023). Tuned Mass Damper Parameters Design by Means of Meta-Heuristic Optimization Algorithms. Civil Engineering and Architecture, 11(3), 1523 - 1537. DOI: 10.13189/cea.2023.110333.*

Abstract Tuned mass dampers (TMDs) as vibration-mitigating devices are widely used in structures to reduce their displacement response under dynamic forces. Through a novel dolphin echolocation (DE) algorithm, this paper provides optimum tuning of TMD parameters. Developing some features of this algorithm results in a faster convergence to the optimum solution. Besides, grey wolf and whale optimization algorithms (GWO and WOA), as two other nature-based meta-heuristic algorithms, are employed in this problem. The modified DE illustrates a more optimum design of TMD's parameters rather than GWO and WOA. The code has been verified by a sample structure from the literature and then applied to a high-rise forty-story structure under strong ground motions. The numerical results reveal that the optimum TMD is viable in attenuating the structural responses, including relative displacements and absolute accelerations under different earthquake excitations. For instance, in the high-rise structure, the modified DE, GWO, and WOA reduce the maximum displacements up to 45%, 43%, and 38%, respectively. Moreover, the algorithms, specifically the modified DE, propose more cost-effective designs in comparison with previous studies in the literature by introducing smaller TMD parameters.

Keywords Seismic Response, Tuned Mass Damper, Multi-Degree of Freedom Structures, Optimization, Meta-Heuristic Algorithms

1. Introduction

Tuned mass dampers (TMDs) are viable means to add additional damping to structures due to their efficiency and low-maintenance cost resulting in the passive control of structures' vibrations created by wind or earthquake excitations. A TMD consists of a mass connecting to a spring and damper. An appropriate tuning reduces dynamic responses of building structures, including relative displacements and absolute accelerations of stories. Ormondroyd and Den Hartog demonstrated that a damper was able to dissipate energy in this configuration leading to a design procedure of TMDs for the first time [1]. Often, TMDs are placed on the roofs of high-rise buildings due to the structures' first-mode shape, where the roof has the most amplitude [2]. Lee et al. installed the TMD on the spatial structure of a rectangular roof [3], and examined the optimum mass ratio and installation location of the TMDs.

The design parameters of TMDs, including frequency and damping ratio, were optimized by Den Hartog for a single degree of freedom (SDOF) structure [4]. McNamara formulated equations of motion and solved them for different input-forcing functions [5]. Response reduction was investigated by variation in the design parameters of the damper. Warburton and Ayorinde illustrated that the optimum parameters of TMDs can be accurately derived for the equivalent SDOF primary system [6]. Tsai and Lin developed a numerical searching procedure to find the optimum tuning frequency and damping ratio of TMDs to a minimum level by proposing an explicit formula [7]. They

also concluded that the TMD was less effective when a high level of damping existed in the primary system. Miranda proposed an energy-based theoretical model for a two-degree-of-freedom (2-DOF) system and demonstrated the system's feasibility for developing substantial damping [8]. Another research by this author introduced some relationships between tuning frequencies and participation factors for a 2-DOF mechanical system [9].

The effectiveness of TMDs was studied in light of energy dissipation and displacement control. Greco and Marano investigated both terms as two objective functions for the optimal design of TMDs [10]. Raggio and De Angelis used the energy-based concept to optimize the design of TMD implemented via inter-story isolation and investigated the seismic performance of the system [11]. Domenico and Ricciardi utilized four different optimization procedures of the TMD in conjunction with the base isolation system [12]. Energy-based measures led to a balanced reduction of both acceleration and displacement of the structures. Tarbali and Nateghi-A examined the TMD's capability of energy absorption and the failure probability of the structure by considering the structural uncertainty [13].

Besides numerical techniques or conventional mathematical methods, determining the optimum parameters of a TMD is an optimization problem that can be solved by the application of optimization algorithms as well. The genetic algorithm proposed by Halland in 1992 has been increasingly applied in engineering fields of study [14], particularly in civil engineering problems [15-19]. This algorithm has also been widely used in finding the optimum parameters of TMDs [20-24]. Colherinhas et al. in 2019 also designed optimum pendulum TMDs in high towers by the genetic algorithm that searched for the minimization of the maximum frequency peaks [25]. Other than the genetic algorithm, many different evolutionary and meta-heuristic algorithms have also been employed to reduce the performance indices of buildings equipped with TMDs. Leung and Zhang proposed a novel particle swarm optimization (PSO) algorithm to minimize some response quantities [26], including the main system's mean square displacement and displacement amplitude under different kinds of excitations. The PSO determined the optimum mass ratio, damping ratio, and tuned frequency. Through a harmony search algorithm (HS), Bekdas and Nigdeli estimated the optimum parameters of TMDs under seismic excitations. [27] The optimization criteria were the peak values of the first story displacement and acceleration transfer function. In another study Bekdas and Nigdeli [28], these researchers considered the soil-structure interaction with high-rise structures and compared the HS and bat algorithms' performance in finding the optimal parameters of TMDs with the objective of maximum displacement minimization. Structures equipped with TMD under continuous stationary critical excitation, i.e., the most severe earthquake, were the subject of Khatibiha et al.'s research [29]. They minimized the root mean square of story drifts by the improved gravitational search algorithm (IGSA). Kaveh et al optimized tuning free parameters of passive and active TMDs by a novel chaotic optimization algorithm (COA) and tested the methodology for a 10-story shear building under strong seismic motions and a 76-story concrete office tower under wind excitation [30]. Of the recent studies, Lara-Valencia et al utilized a novel whale optimization algorithm (WOA) to improve the seismic safety of structures with TMDs [31]. The objective function was the maximum horizontal peak displacement, and root means square (RMS) response of displacements.

Dolphin echolocation (DE) by Kaveh and Farhoudi [32], grey wolf optimizer (GWO) by Mirjalili et al. [33], and whale optimization algorithms (WOA) by Mirjalili and Lewis [34] are three nature-based meta-heuristic algorithms, which have been previously employed to solve complex engineering problems [35-38]. The similarity of these algorithms is that they consist of a group of search agents that randomly explore the search area. The difference is the specifications of mathematical formulations and searching rules. This characteristic makes them different in convergence speed and finding the optimal solution for any specific problems. Recently, many attempts have been performed to improve the mentioned algorithms' performance in each specific problem to avoid getting stuck in local optima and get a faster convergence speed. [39] proposed a modified GWO for global engineering problems. [40] used a modified DE algorithm in order to find the optimum design of steel plate shear walls size and layout [41] and applied a modification in WOA for the problem of structural optimization based on the tent chaotic mapping.

In this research, a novel modified dolphin echolocation algorithm (modified DE) is proposed to investigate the TMD's optimum parameters in reducing the structural responses. As a well-known and viable algorithm, the DE is developed to enhance its specific features in terms of exploration and exploitation phases in a nature-based meta-heuristic algorithm. GWO and WOA, two other similar algorithms, are also selected to compare the results in the optimum value determination and speed of convergence to the ultimate solution (Section 2). Afterwards, the formulation of dynamic equations of motion is derived and assigned to the algorithms by defining a fitness function. A transfer function is defined in the fitness function for the acceleration determination of each story besides considering the displacement directly in the formulation (Section 3). Then, a verification model is adopted to validate the efficiency of the proposed code. Eventually, the design is extended to a high-rise building to demonstrate the efficiency of the proposed approach in other structures and under near-field ground motions (Section 4). The concluding remarks are also declared in Section 5.

2. Optimization Algorithms

This section discusses modifications of the DE algorithm alongside a brief review of GWO and WOA algorithms procedures.

2.1. Modified DE Algorithm

In the following, the modified DE procedure is explained.

- Randomly assign NL locations are assigned randomly in the first step.
- A pre-defined probability (PP) of the existing iteration is denoted by Equation 1.

$$\mathrm{PP}(\mathrm{L_i}) = \mathrm{PP_1} + (1 - \mathrm{PP_1}) \frac{\mathrm{L_i^{Power}}}{(\mathrm{Loops\ Number})^{\mathrm{Power}-1}} \quad (1)$$

Where (PP_1) is the first loop. Changing the power of Equation 1 with 200 number of loops is presented in Figure 1.

The fitness function of all locations is measured, in which superior responses achieve higher probabilities than others.

The fitness of all locations is allocated to other good responses using a symmetric triangular distribution of Figure 2 (Re is the number of affected neighbors). In other words, a coefficient (c) is determined from the following figure, multiplies the current fitness, and sums with the accumulated function, which is derived from the next step.

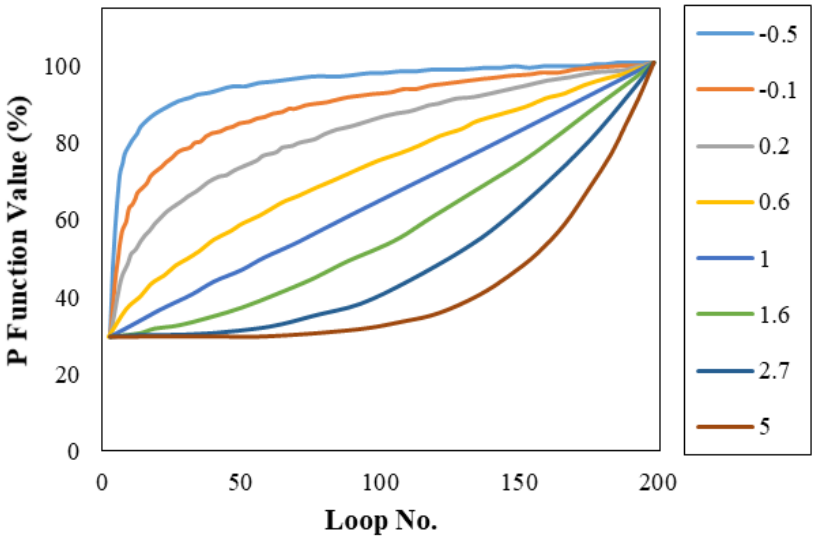

Figure 1. PP vs loop number in Equation 1

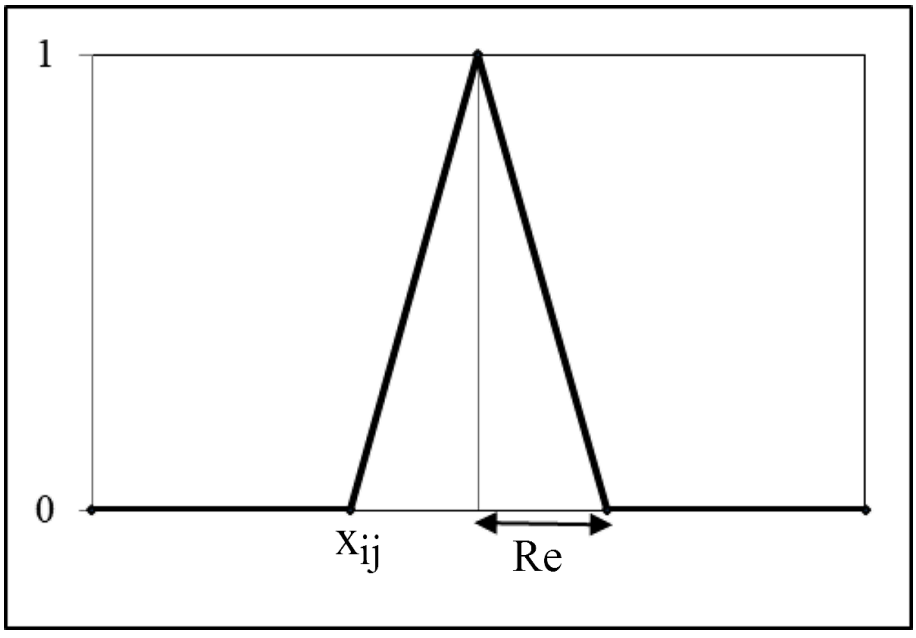

Figure 2. Probability allocation of fitness for i_{th} variable of j_{th} location

- Create accumulative fitness (AF) by adding all dedicated finesses to each variable of each location. Then, a small value of (ε) is added to AF. This action postpones the local optimal solution.

$$AF = AF + \varepsilon \tag{3}$$

- After examining the best location, the corresponding (AF) is set to zero. Then, the probability is measured by normalizing (AF) according to Equation 4.

$$P_{ij} = \frac{AF_{ij}}{\sum_{i=1}^{\text{MaxAj}} AF_{ij}} \tag{4}$$

Where (AF_{ij}) is the accumulative fitness, (Max_{Aj}) is the maximum number of alternatives, and (P_{ij}) is the probability of the i_{th} alternative in the jth dimension.

For the next iteration, ($PP(Loop_i)$) are measured from the best location dimensions. Then, the same process occurs again until reaching the termination criteria.

In the process of coding the algorithm, different parameters should be taken carefully. For instance, the loop number, the convergence curve (the power of Equation 1), the effective radius (Re), the number of locations, and the probability of the first loop. Besides, a fitness function is needed to be defined by the operator for the evaluation process of the algorithm.

Generally, two critical phases exist in any meta-heuristic algorithm: 1) exploration and 2) exploitation. The difference between algorithms is the application of different mathematical formulations for these two phases. Furthermore, the exploration and exploitation phases may not be balanced in an algorithm, which can cause a very popular problem of local optima stuck of the solution. In the DE algorithm, the exploration phase is dominant, resulting in the slow convergence speed to the optimum solution. In order to enhance the exploitation phase of the algorithm and balance it with the exploration phase, a modification is made to the bilinear function of Figure 2. The function corresponding to this figure is as follows:

$$c = 1 - \frac{|x|}{R_e} \tag{5}$$

According to Figure 2, x is defined between ($-R_e$) and ($+R_e$). The peak value for the coefficient (c) is 1. In order to assign larger values for the neighbors of the fitness, a nonlinear function could be defined to modify the exploitation phase of the algorithm. Four functions, which are plotted in Figure 3, are adopted to investigate their effects according to the following equations:

$$c = 1 - \frac{|x|^2}{{R_e}^2} \tag{6}$$

$$c = 1 - \frac{|x|^3}{{R_e}^3} \tag{7}$$

$$c = 1 - \frac{\sqrt{{R_e}^2 - (|x| - R_e)^2}}{R_e} \tag{8}$$

$$c = e^{-6.25(\frac{x}{R_e})^2} \tag{9}$$

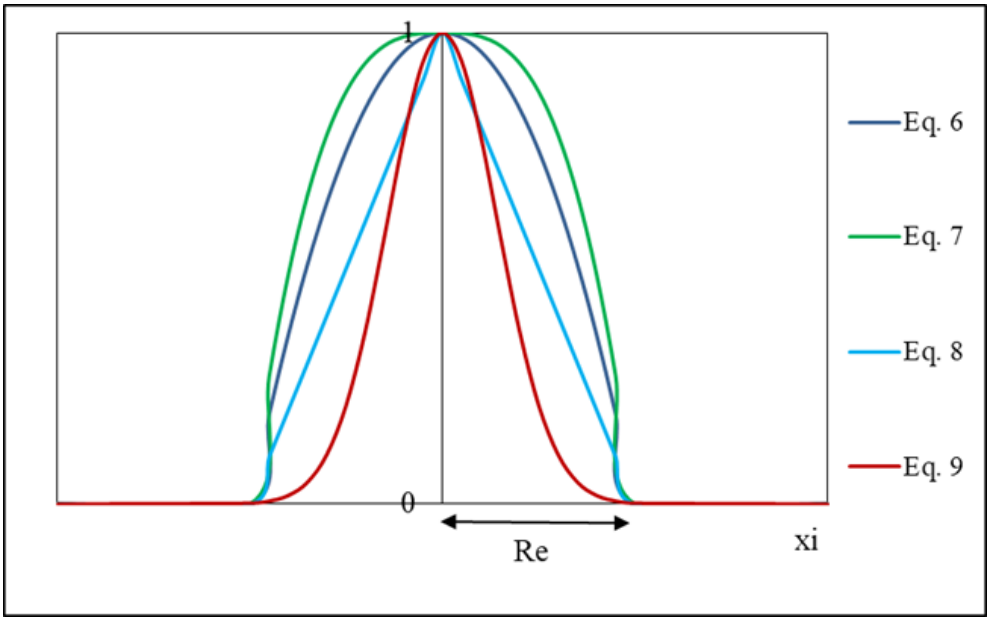

Figure 3. Distribution of fitness with different equations

By examining the current problem with these four functions in addition to the default linear equation, the best results are obtained using Equations 8 and 9.

The next modification of the DE algorithm is related to random selection. [42] demonstrated that the chaotic maps have similar randomness properties compared to the uniform probability distribution of most meta-heuristic algorithms. Hence, a Logistic map [43] is employed in modified DE to improve the algorithm's convergence rate. By this modification, the algorithm employs the following equation to calculate the location of the next step according to the attributed probabilities of each variable:

$$x^{i+1} = 4x^{i}(1 - x^{i}) \tag{10}$$

2.2. GWO Algorithm

Grey wolves are group hunters who are ranked based on their dominancy in four categories as Figure 4.

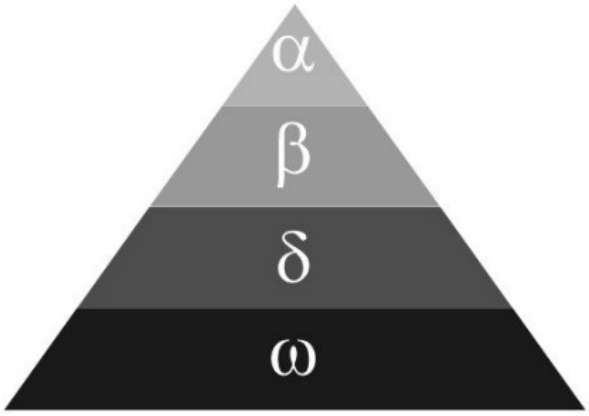

Figure 4. Ranking pyramid of wolves [33]

Alphas are leaders who dictate their decisions to the herd. Betas are the second rank of wolves who help Alphas in leadership. Omegas have the lowest rank and have to follow other wolves. The remaining wolves are Deltas. Delta wolves just follow Alpha and Beta. This group follows some steps for hunting preys by tracing and getting closer to the target, making the target tired and then attack toward it.

This hunting strategy is coded by mathematics since the behavior is similar to solving an optimization problem. In this algorithm, the superior responses are ranked as the Alpha, Beta and Delta, in order, and the remaining are assumed as Omega. As a result, the first three responses are saved as the best response candidates, while other responses need to reform their position based on the updated position of the superior response.

Overall, the exploration phase starts with a random population (as in other algorithms). Alpha, Beta, and Delta find the probable locations of the target. Afterwards, each response reforms its distance from the target. The equations corresponding to the mentioned process are summarized as follows:

$$\vec{G} = \left|\vec{F}.\vec{X}_p(t) - \vec{X}(t)\right| \tag{11}$$

$$\vec{X}(t+1) = \vec{X}_p(t) - \vec{H}.\vec{G} \tag{12}$$

$$\vec{H} = 2\vec{k}.\vec{r}_1 - \vec{k} \tag{13}$$

$$\vec{F} = 2.\vec{r}_2 \tag{14}$$

$$\vec{G}_\alpha = \left|\vec{F}_1.\vec{X}_\alpha - \vec{X}\right|, \vec{G}_\beta = \left|\vec{F}_3.\vec{X}_\beta - \vec{X}\right|, \vec{G}_\delta = \left|\vec{F}_3.\vec{X}_\delta - \vec{X}\right| \tag{15}$$

$$\vec{X}_1 = \vec{X}_\alpha - \vec{H}_1.(\vec{G}_\alpha), \vec{X}_2 = \vec{X}_\beta - \vec{H}_2.(\vec{G}_\beta), \vec{X}_3 = \vec{X}_\delta - \vec{H}_3.(\vec{G}_\delta) \tag{16}$$

$$\vec{X}(t+1) = \frac{\vec{X}_1 + \vec{X}_2 + \vec{X}_3}{3} \tag{17}$$

In these equations: $(\vec{\mathbf{H}})$ and $(\vec{\mathbf{F}})$ are the coefficient vectors determined based on Equations 13 and 14, in which (k) is reduced from two to zero within the iteration process; $(\vec{\mathbf{X}}_\mathbf{p})$ is the prey position and $(\vec{\mathbf{X}})$ is the animal position; $(\vec{\mathbf{r}}_\mathbf{1})$ and $(\vec{\mathbf{r}}_\mathbf{2})$ are random vectors varying from zero to one. In Equation 17, the position vector of wolves is reformed.

2.3. WOA Algorithm

The whales are known as great hunters and the largest mammals in the world. The whales have a tremendous hunting method, in which the exploration for the target is performed by creating circle-like bubbles. This behavior is simulated as an optimizer tool. The animals can find the position of the target encircling the area and assume the target prey as the optimum candidate solution. After finding the best response, other values reform their positions based on the current best value. To begin the formulations, the following can be considered:

$$\vec{G} = \left|\vec{F}.\overrightarrow{X^*}(t) - \vec{X}(t)\right| \tag{18}$$

$$\vec{X}(t+1) = \overrightarrow{X^*}(t) - \vec{H}.\vec{G} \tag{19}$$

Where $(\overrightarrow{\mathbf{X}^*})$ is the best response position vector, $\vec{\mathbf{X}}$ is the location vector, and $(\overrightarrow{\mathbf{X}^*})$ is the reformed position. $(\vec{\mathbf{H}})$ and $(\vec{\mathbf{F}})$ are coefficient vectors derived as follows:

$$\vec{H} = 2\vec{k}.\vec{r} - \vec{a} \tag{20}$$

$$\vec{F} = 2.\vec{r} \tag{21}$$

In these relations, $(\vec{\mathbf{k}})$ is linearly reduced from two to zero during the iteration process, and $(\vec{\mathbf{r}})$ is a random vector in the range of zero to one. The bubble-creating behavior can be designed according to two approaches as follows:

The contraction procedure: when the value of $(\vec{\mathbf{a}})$ is decreased in Equation 20, this phenomenon is simulated.

Reforming the spiral formations: when the distance is whale and the target is calculated, the updating process occurs. Note that the (X, Y) and (X^*,Y^*) are the whale and prey locations respectively.

$$\vec{X}(t+1) = \overrightarrow{G'}.e^{bl}.\cos(2\pi l) + \overrightarrow{X^*}(t) \quad (22)$$

Where $\overrightarrow{G'} = |\overrightarrow{X^*}(t) - \vec{X}(t)|$, (b) is constant for spiral logarithmic formation, and l is a random number in [-1,+1].

To perform a global search, the variation of $(\vec{H})$, and $(|\overrightarrow{A}| > 1)$ enables the agent's whales to search randomly the surrounding area with the aid of the following equation:

$$\vec{G} = \left|\vec{F}.\overrightarrow{X_{rand}} - \vec{X}\right| \quad (23)$$

$$\vec{X}(t+1) = X_{rand} - \vec{H}.\vec{G} \quad (24)$$

Where $(\mathbf{X_{rand}})$ is the position vector selected randomly. Based on the above-mentioned strategy, the WOA algorithm is assumed as a global optimizer, where it utilizes the neighbors of the best solution to the convergence process.

3. Equations of Motion and Optimization Process

As mentioned earlier, the optimum parameters of a TMD consist of the mass, the damping ratio, and the system's frequency. In order to improve the TMD's performance against seismic excitations, optimum tuning of these parameters is desired. However, this optimized system must satisfy the structural constraints, including story drifts and displacements. A multi-degree of freedom (MDOF) system with a TMD on the top floor is depicted in Figure 5. The dynamic equation of motion is as follows:

$$\mathbf{M\ddot{x}}(t) + \mathbf{C\dot{x}}(t) + \mathbf{Kx}(t) = -\mathbf{Mr\ddot{x}_g} + \mathbf{f} \quad (25)$$

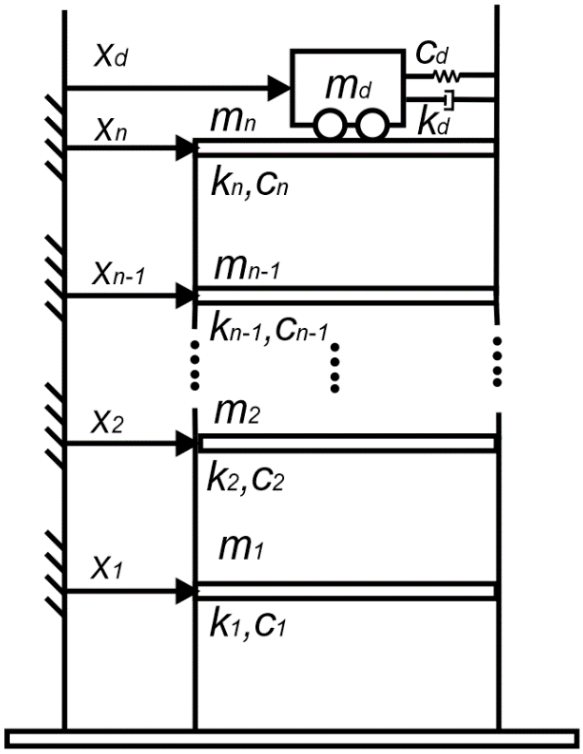

Figure 5. MDOF system with TMD on the top floor

Where (M), (C), (K) are matrices of mass, stiffness, and damping of the MDOF structure. $(\ddot{\mathbf{x}}(t))$, $(\dot{\mathbf{x}}(t))$, and $(\mathbf{x}(t))$ are vectors of the relative acceleration, velocity and the displacement of the structure, respectively. (r) is the influence vector of ground accelerations $(\ddot{\mathbf{x}}_\mathbf{g})$, and (f) is the applied forces on each floor.

$$M = \begin{bmatrix} m_1 & 0 & 0 & 0 & 0 \\ 0 & m_2 & 0 & 0 & 0 \\ \cdots & \cdots & \ddots & \cdots & \cdots \\ 0 & 0 & 0 & m_n & 0 \\ 0 & 0 & 0 & 0 & m_d \end{bmatrix} \quad (26)$$

$$C = \begin{bmatrix} (c_1 + c_1) & -c_2 & 0 & 0 & 0 \\ -c_2 & (c_2 + c_3) & 0 & 0 & 0 \\ \cdots & \cdots & \ddots & \cdots & \cdots \\ 0 & 0 & 0 & (c_n + c_d) & -c_d \\ 0 & 0 & 0 & -c_d & c_d \end{bmatrix} \quad (27)$$

$$K = \begin{bmatrix} (k_1 + k_1) & -k_2 & 0 & 0 & 0 \\ -k_2 & (k_2 + k_3) & 0 & 0 & 0 \\ \cdots & \cdots & \ddots & \cdots & \cdots \\ 0 & 0 & 0 & (k_n + k_d) & -k_d \\ 0 & 0 & 0 & -k_d & k_d \end{bmatrix} \quad (28)$$

$$x(t) = [\ x_1 \quad x_2 \quad \cdots \quad x_n \quad x_d\ ]^T \quad (29)$$

$$f = [\ f_1 \quad f_2 \quad \cdots \quad f_n \quad f_d\ ]^T \quad (30)$$

$$r = [\ 1 \quad \cdots \quad 1\ ]^T \quad (31)$$

Where (m_i), (c_i), (k_i), and (x_i) are mass, damping coefficient, stiffness, and horizontal displacement of the i_{th} story of the building (i=1, 2, …, n). (m_d), (c_d), and (k_d) are the mass, damping ratio, and the stiffness of the TMD, respectively. (x_d) and (f_d) are the TMD's relative displacement to the ground, and the external force applied to the damper. Converting the equation of motion to the state-space form results in the following equation:

$$\dot{\mathbf{Z}}(\mathrm{t}) = \mathbf{AZ}(\mathrm{t}) + \mathbf{BU}(\mathrm{t}) \tag{32}$$

$$\mathbf{y} = \ddot{\mathbf{x}}(\mathbf{t}) + \mathbf{r}\ddot{\mathbf{x}}_\mathbf{g} = [-\mathbf{M^{-1}K} \quad -\mathbf{M^{-1}C}]\begin{bmatrix}\mathbf{x(t)}\\ \dot{\mathbf{x}}(\mathbf{t})\end{bmatrix} + \mathbf{M^{-1}f} \tag{33}$$

Where y is the vector formed by absolute accelerations. (A), (B), (Z(t)) and $(U(t))$ are system matrices by the following equations ($\mathbf{0}$ and $\boldsymbol{I}$ are zero and identity matrices):

$$\mathbf{A} = \begin{bmatrix}\mathbf{0} & \mathbf{I}\\ -\mathbf{M^{-1}K} & -\mathbf{M^{-1}C}\end{bmatrix} \tag{34}$$

$$\mathbf{B} = \begin{bmatrix}\mathbf{0} & \mathbf{0}\\ -\mathbf{r} & \mathbf{M^{-1}}\end{bmatrix} \tag{35}$$

$$\mathbf{Z(t)} = \begin{Bmatrix}\mathbf{x(t)}\\ \dot{\mathbf{x}}(\mathbf{t})\end{Bmatrix} \tag{36}$$

$$\mathbf{U(t)} = \begin{Bmatrix}\ddot{\mathbf{x}}_\mathbf{g}\\ \mathbf{f}\end{Bmatrix} \tag{37}$$

In this study, TMD is located at the top floor, which makes the components of the vector (f) zero except the last component that is the last degree of freedom as defined above.

The optimization goal is minimizing the maximum Frequency Response Functions (FRFs). Accordingly, the responses must be defined at the frequency domain. The transfer function of this problem, which is depicted in Figure 6, is as follows:

$$\begin{bmatrix}\mathrm{Y_1(s)}\\ \mathrm{Y_2(s)}\\ \cdots\\ \mathrm{Y_n(s)}\end{bmatrix} = \begin{bmatrix}\mathrm{G_{11}(s)} & \mathrm{G_{12}(s)} & \cdots & \mathrm{G_{1n}(s)} & \mathrm{G_{1d}(s)}\\ \mathrm{G_{21}(s)} & \mathrm{G_{11}(s)} & \cdots & \mathrm{G_{11}(s)} & \mathrm{G_{2d}(s)}\\ \cdots & \cdots & \ddots & \cdots & \cdots\\ \mathrm{G_{n1}(s)} & \mathrm{G_{n2}(s)} & \cdots & \mathrm{G_{n3}(s)} & \mathrm{G_{nd}(s)}\end{bmatrix}\begin{bmatrix}\mathrm{F_1(s)}\\ \mathrm{F_2(s)}\\ \cdots\\ \mathrm{F_n(s)}\\ \mathrm{F_d(s)}\end{bmatrix} \tag{38}$$

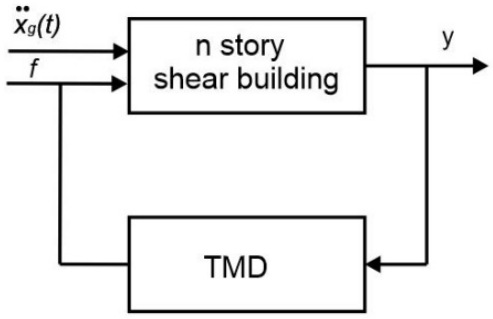

Figure 6. Schematic of the framework

Where $(Y_i(s))$, $(F_i(s))$, and $(F_d(s))$ are the Laplace transform of (y_i), (f_i), and $(\ddot{x}_g)$, respectively. $(G_{ij}(s))$ is the transfer function between the measured acceleration at ith floor and the force applied to the jth floor (i,j=[1,n]), and $(G_{id}(s))$ is the transfer function between the acceleration measured at ith floor and the ground acceleration $(\ddot{x}_g)$. Thus, the objective function of this problem is to find the optimum values of TMD's stiffness and damping ratio by minimizing the following equation:

$$\text{objective function} = \frac{\max|\mathrm{x_1}^{\mathrm{TMD}}|}{\max|\mathrm{x_1}^{\mathrm{No\ TMD}}|} + \frac{\max|\mathrm{G_{y_1}}^{\mathrm{TMD}}|}{\max|\mathrm{G_{y_1}}^{\mathrm{No\ TMD}}|} \tag{39}$$

Where $(x_1{}^{TMD})$ and $(x_1{}^{No\ TMD})$ are the displacements of the first story with and without TMD. (G) is the transfer function i.e., the ratio of the Laplace transformation of each story's acceleration and the ground acceleration. $(G_{y_1}{}^{TMD})$ and $(G_{y_1}{}^{No\ TMD})$ are the transfer functions of the first story with and without TMD.

4. Numerical Examples

This section investigates two different case studies to verify the written code and compare the performance of modified DE, GWO, and WOA algorithms.

4.1. Example One

The workability of the proposed algorithms is investigated by a sample shear building with ten stories. The story's mass is lumped on each floor. The specifications of the building are shown in Table 1.

Table 1. Details of the building of example one

Story mass (ton)	Story stiffness (kN/m)	Story damping (kN.s/m)	Damper mass (ton)
360	650000	6200	108

The optimum values of stiffness and damping of the damper are the goal of this example, shown in Table 2, and compared with two other studies. Hadi and Arfiadi (1998) and Kaveh et al. (2020) applied the genetic algorithm (GA) and chaotic optimization algorithm (COA), respectively, to find the optimum values of the damper's stiffness and damping. This table shows a good correlation between the former results and the newly obtained by modified DE, GWO, and WOA. The building is subjected to the El Centro earthquake (1940), and the displacement results, in the absence and presence of TMD, are derived based on the optimum TMD values determined by algorithms. The peak displacements and the reduction of displacements are determined for each story and compared with the mentioned studies (Table 3). The reduction range is from 34% to 40% for all three algorithms (modified DE, GWO, and WOA), which is close to the determined values by the genetic and chaotic optimization algorithms. Accordingly, the modified DE resulted in more reduction of stories' displacement than WOA, GA, and COA. However, GWO is better matched with modified DE results.

Table 2. Optimum parameters of TMD in example one compared to previous studies

TMD parameters	GA [44]	COA [33]	Modified DE (present study)	GWO (present study)	WOA (present study)
Stiffness (kN/m)	3750	3653.9	3922.2	3722.0	4115.1
Damping (kN.s/m)	151.5	121.5	209.4	169.2	268.6

Table 3. Maximum and the reduction of stories displacement under El Centro earthquake

Story	Displacement (no TMD)	Displacement (m)-Reduction (%)				
		GA	COA	Modified DE	GWO	WOA
1	0.031	0.019-38.71	0.019-38.71	0.019-38.71	0.019-38.71	0.020-35.84
2	0.060	0.037-38.33	0.037-38.33	0.037-38.33	0.037-38.33	0.039-35.00
3	0.087	0.058-33.33	0.053-39.08	0.053-39.08	0.054-37.93	0.057-34.48
4	0.112	0.068-39.29	0.068-39.29	0.068-39.28	0.068-39.28	0.071-36.60
5	0.133	0.082-38.35	0.081-39.10	0.083-37.59	0.083-37.59	0.085-36.09
6	0.151	0.094-37.75	0.093-38.41	0.092-39.07	0.093-38.41	0.096-36.42
7	0.166	0.104-37.35	0.103-37.95	0.103-37.95	0.103-37.95	0.106-36.14
8	0.177	0.113-36.16	0.112-36.72	0.111-37.29	0.112-36.72	0.113-36.16
9	0.184	0.119-35.35	0.118-35.87	0.116-36.96	0.118-35.87	0.120-34.78
10	0.188	0.122-35.11	0.121-35.64	0.121-35.64	0.121-35.64	0.122-35.11

4.2. Example Two

The second example is a high-rise building with 40 stories and a TMD on the top floor studied by [45] and 46], who respectively used ant colony optimization (ACO) and particle swarm optimization (PSO) algorithms for the parameter identification of the current problem. The specifications of this sample building are shown in Table 4.

In this example, a complete design of the TMD system includes the TMD's mass other than its stiffness and damping coefficient. The designed parameters based on the three algorithms of the present study (modified DE, GWO, and WOA algorithms) are shown in Table 5 and compared to other studies [45] and [46]. The modified DE designed the TMD's parameters in a way that the fitness function in Equation 39 converged to a more optimum solution in comparison with GWO and WOA (present study), ACO [45], and PSO [46]. The reduction percentage of mass was 3.9%, 2.1%, and 1.9% in modified DE, GWO, and WOA, while the reduction percentage of stiffness was 40.2%, 31.3%, and 10.0% for the mentioned algorithms, respectively. This achievement explicates that the modification applied to the DE algorithm made exploration and exploitation phases more effective considering the similar nature of the three applied algorithms. Besides, the convergence speed of modified DE is less than the two other algorithms. In this regard, other studies that used this algorithm reported that the DE speed of convergence is usually less than similar meta-heuristic algorithms due to the probability assigned to each response in each step of iteration [38], which is novel among these types of algorithms. Through the modification in this study, the convergence speed was increased, and the latter-mentioned privilege was maintained simultaneously.

The 1978 TABAS earthquake, Iran (RSN 143, TABAS station) is applied to the structure, similar to the mentioned studies. In order to compare the results with the previous studies, the relative displacements are compared in this example. With this earthquake, ACO and PSO revealed a 30.14% and 35.96% reduction in the maximum relative displacement of the structure. However, applying the modified DE in the present study resulted in more reduction of this parameter with a value of 41.26%. In this regard, GWO and WOA showed 35.11% and 33.67% reduction of the maximum relative displacement, respectively. Figure 7 illustrates the relative displacement of the 40th story under the TABAS earthquake in the presence and absence of TMD in all three algorithms. Generally, the top story displacement is critical in tall buildings, and this figure accurately displays the viable solution of a TMD in peak displacement reduction. However, the maximum relative displacement under the

TABAS earthquake for all stories is presented in Table 6. According to this table, a TMD system is effective in relative displacement reduction of all stories. Notwithstanding, the reduction is greater for top stories than others at the bottom. This table also compares the performance of the algorithms used in this study and the studies mentioned earlier. The modified DE algorithm demonstrated better performance in designing the TMD system, resulting in more displacement reductions. Although the GWO and WOA algorithms are working properly with adequate efficiency, their results in displacement reduction were similar to the previous study by [45] PSO. The results derived by [46] for the optimum TMD revealed an over-design in comparison with the PSO [46], modified DE, GWO, and WOA of the present study.

Table 4. Specifications of the structure in example two

TMD parameters	GA [44]	COA [33]	Modified DE (present study)	GWO (present study)
Stiffness (kN/m)	3750	3653.9	3922.2	3722.0

Table 5. Optimum parameters of TMD

TMD parameters	ACO [45]	PSO [46]	Modified DE (present study)	GWO (present study)	WOA (present study)
Stiffness (kN/m)	3037.97	2330.44	2097.97	2347.01	2808.90
Damping (kN.s/m)	173.50	91.45	103.73	119.21	156.18
Mass (ton)	1547.72	1515.05	1487.95	1514.89	1518.90

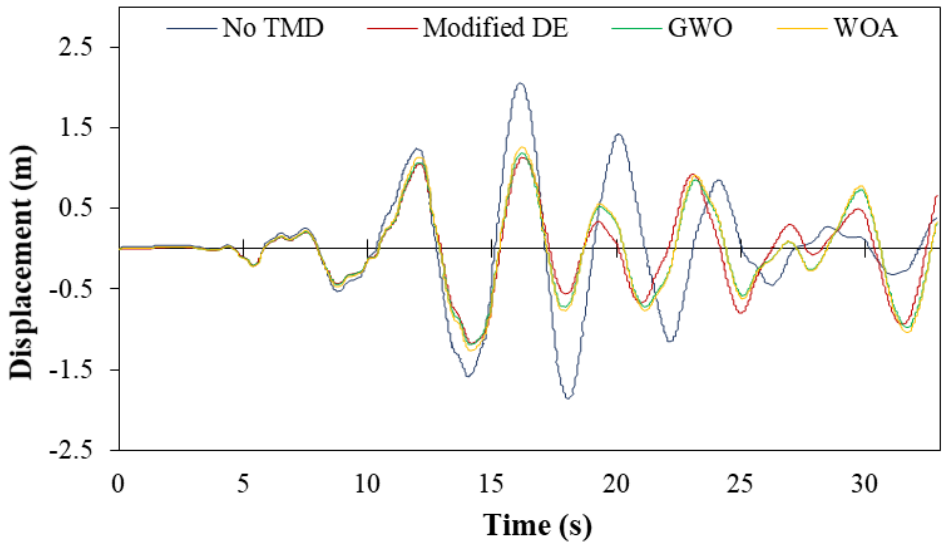

Figure 7. Relative displacement of 40-story building of example two under TABAS earthquake

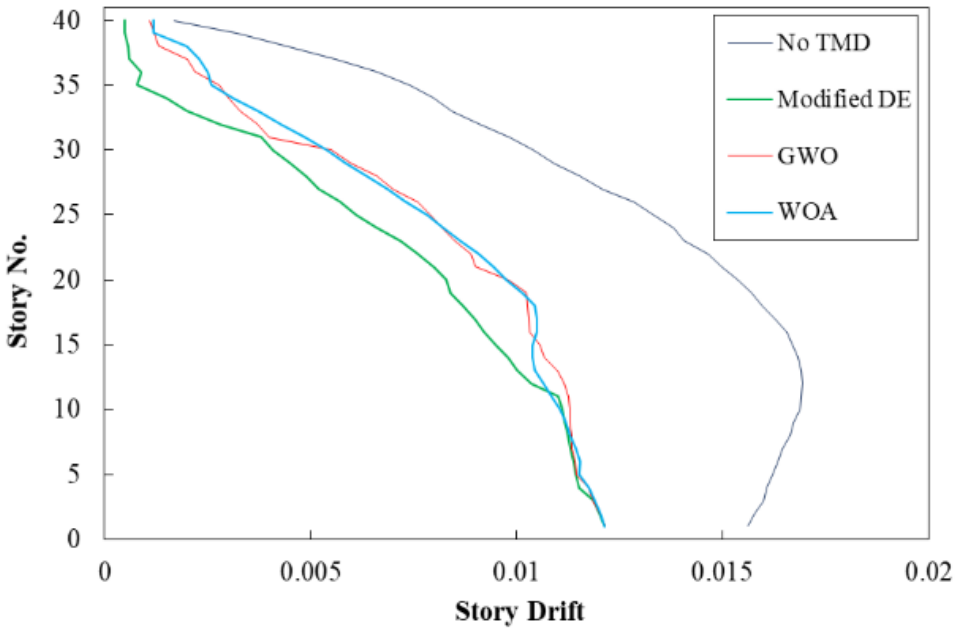

Figure 8. Story drifts in example two under TABAS earthquake by different algorithms

Afterward, the story drift as a crucial parameter in design considerations is calculated for all stories and is depicted in Figure 8 for all applied algorithms. According to this figure, story drift values are in a narrow band for all algorithms, specifically for the modified DE. This manifests a uniform distribution of the constraint of the problem, which means a similar contribution of building displacement control as an optimum solution.

Last but not least, three earthquakes are applied to this structure, first in the absence and then in the presence of the optimally designed TMD, in order to study the efficiency of the designed system. The selected records are near-field earthquakes of Chi-Chi, Kobe, and Northridge due to the severe ground motion, affecting the structure. The displacements are depicted in Figures 9, 10, and 11 for Chi-Chi, Kobe, and Northridge records, respectively. The strength of the TMD application can be observed in these figures for different severe ground motions. In order to compare the relative displacements quantitatively determined by different algorithms, the maximum relative displacements of all analyzes are shown in Table 7. The reduction of maximum displacement is 35.05%, 44.44%, and 41.58% for three earthquakes of Chi-Chi, Kobe, and Northridge, respectively, by the modified DE design of TMD. Nevertheless, this reduction is also in an appropriate range of 27%-42% for other algorithms. Consequently, The DE algorithm is capable of designing more economical systems with less computational effort by modifying some features of the algorithm in this problem. Table 8 also demonstrates that the TMD also has a positive effect on the maximum acceleration reduction of the structure.

Table 6. Maximum relative displacement of all stories in example two under TABAS earthquake by different algorithms

Story	Displacement (no TMD)	Displacement (m)-Reduction (%)			
		PSO	Modified DE	GWO	WOA
1	0.0626	0.0486-22.36	0.0485-22.52	0.0486-22.36	0.0486-22.36
2	0.1259	0.0967-23.19	0.0965-23.35	0.0967-23.19	0.0968-23.11
3	0.1898	0.1443-23.97	0.1440-24.17	0.1441-24.08	0.1443-23.97
4	0.2542	0.1913-24.74	0.1901-25.22	0.1911-24.82	0.1911-24.82
5	0.3191	0.2374-25.60	0.2358-26.10	0.2369-25.76	0.2370-25.73
6	0.3844	0.2828-26.43	0.2762-28.15	0.2801-27.13	0.2819-26.67
7	0.4500	0.3272-27.29	0.3194-29.02	0.3260-27.56	0.3271-27.31
8	0.5162	0.3708-28.17	0.3636-29.56	0.3701-28.30	0.3701-28.30
9	0.5827	0.4144-28.88	0.4063-30.29	0.4112-29.43	0.4132-29.09
10	0.6497	0.4577-29.55	0.4512-30.55	0.4515-30.51	0.4571-29.64
11	0.7171	0.5000-30.28	0.4921-31.38	0.4996-30.33	0.4998-30.30
12	0.7847	0.5413-31.02	0.5411-31.04	0.5386-31.36	0.5409-31.07
13	0.8523	0.5814-31.87	0.5786-32.11	0.5777-32.22	0.5798-31.97
14	0.9198	0.6208-32.51	0.6193-32.67	0.6196-32.64	0.6196-32.64
15	0.9869	0.6626-32.86	0.6522-33.91	0.6588-33.24	0.6609-33.03
16	1.0533	0.7065-32.93	0.7060-32.97	0.7057-33.00	0.7068-32.90
17	1.1182	0.7493-32.99	0.7480-33.11	0.7485-33.06	0.7490-33.02
18	1.1821	0.7911-33.08	0.7876-33.37	0.7891-33.25	0.7915-33.04
19	1.2446	0.8317-33.18	0.8311-33.22	0.8309-33.24	0.8326-33.10
20	1.3056	0.8707-33.30	0.8656-33.70	0.8676-33.55	0.8736-33.09
21	1.3646	0.9085-33.42	0.8967-34.29	0.8967-34.29	0.9096-31.88
22	1.4217	0.9448-33.54	0.9326-34.40	0.9376-34.05	0.9468-33.40
23	1.4770	0.9794-33.69	0.9701-34.32	0.9723-34.17	0.9822-33.50
24	1.5303	1.0122-33.86	0.9911-35.23	0.9956-34.94	1.0130-33.80
25	1.5814	1.0435-34.01	1.0121-36.00	1.0210-35.44	1.0439-33.99
26	1.6303	1.0727-34.20	1.0672-33.99	1.0703-34.35	1.0739-34.13
27	1.6765	1.1002-34.38	1.0713-36.10	1.0941-32.95	1.1103-33.77
28	1.7205	1.1257-34.57	1.0802-37.22	1.1126-35.33	1.1259-34.56
29	1.7623	1.1491-34.80	1.1259-36.11	1.1349-35.60	1.1526-34.60
30	1.8016	1.1707-35.02	1.1351-36.99	1.1600-35.61	1.1784-34.58
31	1.8385	1.1901-35.72	1.1720-36.25	1.1863-35.47	1.1956-34.97
32	1.8727	1.2072-35.54	1.1822-36.87	1.1940-36.24	1.2109-35.44
33	1.9041	1.2221-35.82	1.2094-36.48	1.2167-36.10	1.2310-35.35
34	1.9324	1.2346-36.11	1.2111-37.33	1.2241-36.65	1.2359-36.04
35	1.9574	1.2448-36.41	1.2199-37.68	1.2358-36.86	1.2489-36.20
36	1.9789	1.2559-36.54	1.2364-37.53	1.2420-37.23	1.2576-36.45
37	1.9965	1.2695-36.41	1.2416-37.83	1.2539-37.19	1.2715-36.31
38	2.0100	1.2816-36.24	1.2587-37.38	1.2696-36.83	1.2868-63.52
39	2.0193	1.2907-36.08	1.2724-36.99	1.2809-36.57	1.2959-35.82
40	2.0241	1.2963-35.96	1.2744-37.04	1.2868-36.43	1.3063-35.46

By employing the design parameters of the TMD determined by modified DE, the absolute acceleration of the structure experienced a 32% reduction in the Northridge record. However, this reduction value is not significant in the Chi-Chi record by under 1% decrease. According to Tables 7 and 8, both displacement and acceleration responses of the structure are significantly increased under the Northridge record compared to

Chi-Chi and Kobe, which demonstrates that the frequency of the excitation might be near the frequency of the structure in the Northridge earthquake. Hence, the building was also capable of reducing the peak responses even when the resonance occurred.

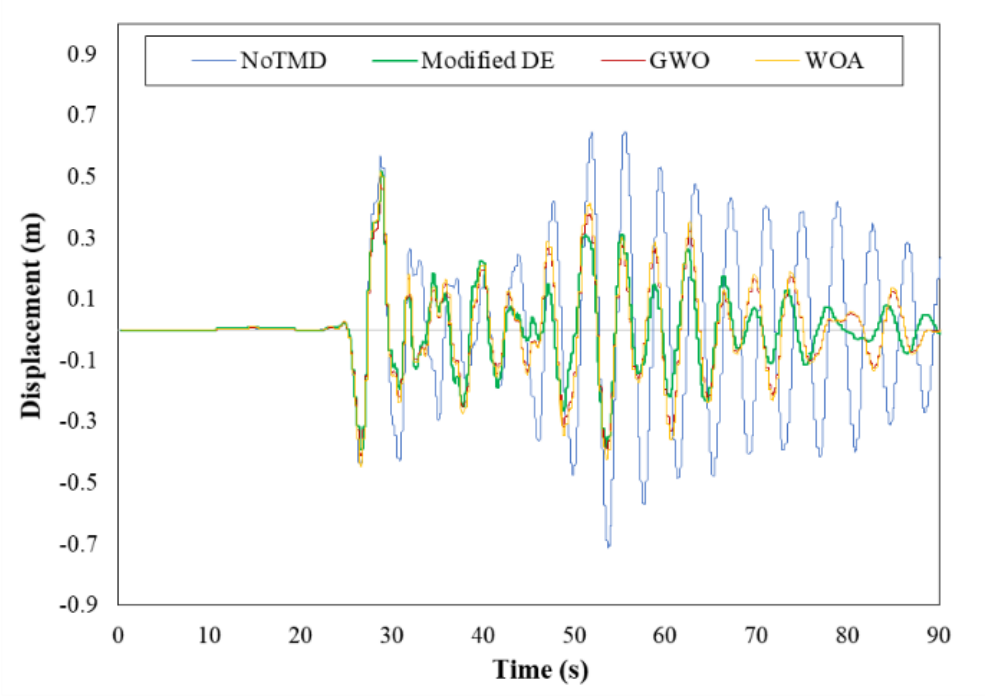

Figure 9. Displacement of 40th story in example two under Chi-Chi record

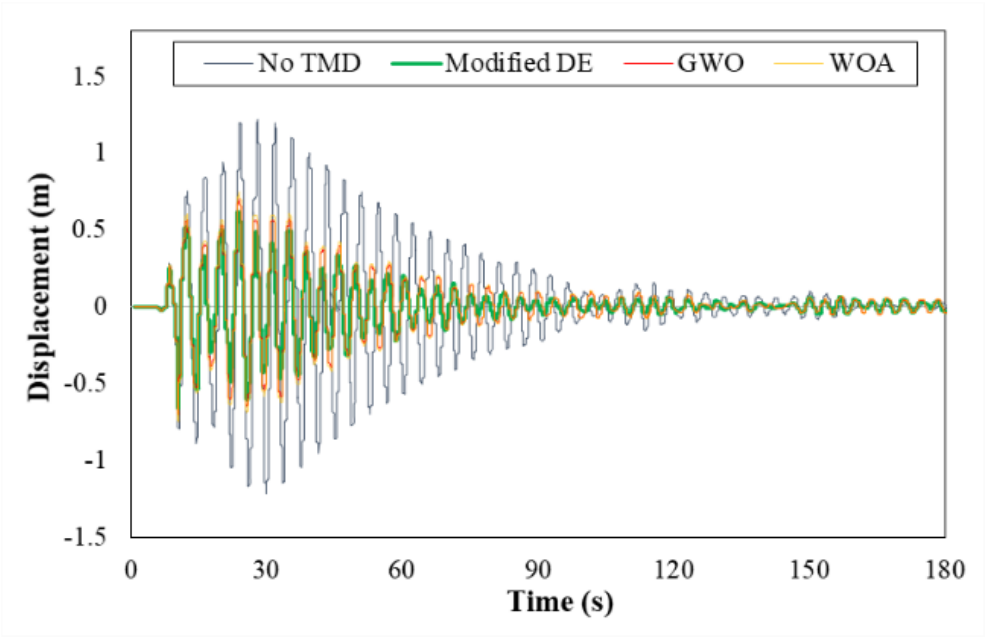

Figure 10. Displacement of 40th story in example two under Kobe record

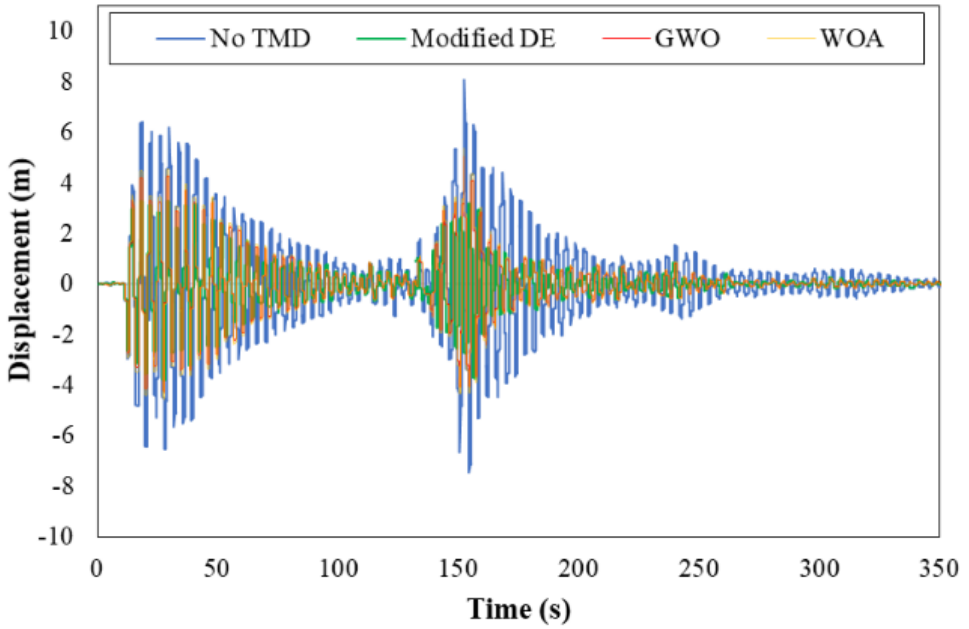

Figure 11. Displacement of 40th story in example two under Northridge record

5. Summary and Conclusion

In structural engineering, three main methods of controlling vibration have been proposed in the literature: active, passive, and semi-active controls. Many devices exist to attenuate oscillation amplitude among these methods, including TMDs, base isolation systems, and viscous dampers. In this study, the optimum design of TMDs as the first objective was investigated, and the following were extracted:

- Three meta-heuristic algorithms with almost the same functions were adopted from the literature, including DE, GWO, and WOA algorithms.
- Probability assignment to each solution is the prominent feature of the DE algorithm. Due to some extra features of DE, which were mentioned in previous studies for many structural engineering problems compared to the two others, a modification was made to this algorithm. A novel modified DE was proposed, which developed some features of this robust algorithm.
- The modification is performed to balance the two phases of the algorithm, which are exploration and exploitation. In this regard, four new formulations are assigned to accumulative fitness, and the best performance is selected for this problem. Besides, a chaotic logistic map is added for random selection. These two modifications boosted the algorithm performance in terms of convergence speed and avoiding local optima.
- The dynamic equations of motion were extracted in the presence and absence of the TMD system for an MDOF structure. A code was written in this regard in state-space condition.
- All three algorithms were defined for the optimum design of TMD's parameters. For this purpose, a fitness function was defined to bridge the dynamic system and algorithms to find the optimum parameters of TMDs.
- The code was verified with other studies in the literature, which resulted in even better performance of TMDs in displacement reduction of the building.
- Afterward, the feasibility of the system was tested in a high-rise structure with all mentioned algorithms under severe ground motions.
- The findings illustrated that the TMD was a reliable system. Besides, modification of the DE algorithm proposed a faster convergence speed than the previous version avoiding getting stuck in local minima.

Table 7. Maximum relative displacement in example two under three earthquakes by different algorithms

Record	Displacement (no TMD)	Displacement (m)-Reduction (%)		
		Modified DE	GWO	WOA
Chi-Chi	0.7050	0.4579-35.05	0.4914-30.30	0.5124-27.32
Kobe	1.2249	0.6805-44.44	0.7015-42.73	0.7642-37.61
Northridge	8.0662	4.7117-41.58	5.1652-35.96	5.4133-32.89

Table 8. Maximum absolute acceleration in example two under three earthquakes by different algorithms

Record	Acceleration (no TMD)	Acceleration (m/s2)-Reduction (%)		
		Modified DE	GWO	WOA
Chi-Chi	7.7407	7.7119-0.37	7.7321-0.86	7.7314-0.93
Kobe	4.9311	4.3328-12.13	4.5996-6.72	4.9111-0.41
Northridge	30.5266	20.9985-32.21	22.1962-27.29	26.8667-11.99

- The exploration and exploitation of the algorithm were also developed, leading to a more economical design of the TMD system compared to other studies and different algorithms employed in the present study.
- The TMD also affected the absolute acceleration other than relative displacements. However, the dominant reduction is for the relative displacements and drift ratios.
- Accordingly, the modified DE can also be tested for other engineering problems to investigate the efficiency of the proposed method for future works.

REFERENCES

[1] Ormondroyd, J. The theory of the dynamic vibration absorber, *Trans., ASME, Applied Mechanics*, *50*, 9-22, 1928

[2] Yucel, M., Bekdaş, G., Nigdeli, S. M., & Sevgen, S. (2019). Estimation of optimum tuned mass damper parameters via machine learning. *Journal of Building Engineering*, *26*, 100847.

[3] Lee, Y. R., Kim, H. S., & Kang, J. W. (2021). Seismic Response Control Performance Evaluation of Tuned Mass Dampers for a Retractable-Roof Spatial Structure. *International Journal of Steel Structures*, *21*(1), 213-224.

[4] J.P. Den Hartog, Mechanical Vibrations, third ed., McGraw-Hill, New York, 1947.

[5] Tsai, H. C., & Lin, G. C. (1993). Optimum tuned‐mass dampers for minimizing steady‐state response of support‐excited and damped systems. *Earthquake engineering & structural dynamics*, *22*(11), 957-973.

[6] McNamara, R. J. (1977). Tuned mass dampers for buildings. *Journal of the Structural Division*, *103*(9), 1785-1798.

[7] Warburton, G. B., & Ayorinde, E. O. (1980). Optimum absorber parameters for simple systems. *Earthquake Engineering & Structural Dynamics*, *8*(3), 197-217.

[8] Miranda, J. C. (2005). On tuned mass dampers for reducing the seismic response of structures. *Earthquake engineering & structural dynamics*, *34*(7), 847-865.

[9] Miranda, J. C. (2016). Discussion of system intrinsic parameters of tuned mass dampers used for seismic response reduction. *Structural Control and Health Monitoring*, *23*(2), 349-368.

[10] Greco, R., & Marano, G. C. (2013). Optimum design of tuned mass dampers by displacement and energy perspectives. *Soil dynamics and earthquake engineering*, *49*, 243-253.

[11] Reggio, A., & Angelis, M. D. (2015). Optimal energy‐based seismic design of non‐conventional Tuned Mass Damper (TMD) implemented via inter‐story isolation. *Earthquake Engineering & Structural Dynamics*, *44*(10), 1623-1642.

[12] De Domenico, D., & Ricciardi, G. (2018). Earthquake-resilient design of base isolated buildings with TMD at basement: Application to a case study. *Soil Dynamics and Earthquake Engineering*, *113*, 503-521.

[13] Tarbali, K., & Nateghi-A, F. (2014). Effect of structural uncertainty on seismic response of steel moment-resisting frames equipped with tuned mass dampers. *International Journal of Steel Structures*, *14*(2), 231-241.

[14] Holland, J. H. (1992). Genetic algorithms. *Scientific american*, *267*(1), 66-73.

[15] Feng, R. Q., Liu, F. C., Xu, W. J., Ma, M., & Liu, Y. (2016). Topology optimization method of lattice structures based on a genetic algorithm. *International Journal of Steel Structures*, *16*(3), 743-753.

[16] Park, J., Chun, Y. H., & Lee, J. (2016). Optimal design of an arch bridge with high performance steel for bridges using genetic algorithm. *International Journal of Steel Structures*, *16*(2), 559-572.

[17] Palizi, S., & Daryan, A. S. (2021). Critical Temperature Evaluation of Moment Frames by Means of Plastic

Analysis Theory and Genetic Algorithm. *Iranian Journal of Science and Technology, Transactions of Civil Engineering*, 1-14.

[18] Saedi Daryan, A., & Palizi, S. (2020). New plastic analysis procedure for collapse prediction of braced frames by means of genetic algorithm. *Journal of Structural Engineering*, *146*(1), 04019168.

[19] Palizi, S., & Toufigh, V. (2022). Bond strength prediction of timber-FRP under standard and acidic/alkaline environmental conditions based on gene expression programming. *European Journal of Wood and Wood Products*, *80*(6), 1457-1471.

[20] Mittal, N., Singh, U., & Sohi, B. S. (2016). Modified grey wolf optimizer for global engineering optimization. *Applied Computational Intelligence and Soft Computing*, *2016*.

[21] Stewart, G., & Lackner, M. (2012). Determining optimal tuned mass damper parameters for offshore wind turbines using a genetic algorithm. In *50th AIAA aerospace sciences meeting including the new horizons forum and aerospace exposition* (p. 376).

[22] Mohebbi, M., & Joghataie, A. (2012). Designing optimal tuned mass dampers for nonlinear frames by distributed genetic algorithms. *The Structural Design of Tall and Special Buildings*, *21*(1), 57-76.

[23] Desu, N. B., Deb, S. K., Dutta, A. (2006). Coupled tuned mass dampers for control of coupled vibrations in asymmetric buildings. Structural Control and Health Monitoring., 13:5, 897–916.

[24] Pourzeynali, S., Lavasani, H. H., Modarayi, A. H. (2007). Active control of high rise building structures using fuzzy logic and genetic algorithms. Engineering Structures. 29:3, 346–357.

[25] Colherinhas, G. B., de Morais, M. V., Shzu, M. A., & Avila, S. M. (2019). Optimal pendulum tuned mass damper design applied to high towers using genetic algorithms: Two-DOF modeling. *International Journal of Structural Stability and Dynamics*, *19*(10), 1950125.

[26] Leung, A. Y. T., & Zhang, H. (2009). Particle swarm optimization of tuned mass dampers. *Engineering Structures*, *31*(3), 715-728.

[27] Bekdaş, G., & Nigdeli, S. M. (2011). Estimating optimum parameters of tuned mass dampers using harmony search. *Engineering Structures*, *33*(9), 2716-2723.

[28] Bekdaş, G., & Nigdeli, S. M. (2017). Metaheuristic based optimization of tuned mass dampers under earthquake excitation by considering soil-structure interaction. *Soil Dynamics and Earthquake Engineering*, *92*, 443-461.

[29] Khatibinia, M., Gholami, H., & Kamgar, R. (2018). Optimal design of tuned mass dampers subjected to continuous stationary critical excitation. *International Journal of Dynamics and Control*, *6*(3), 1094-1104.

[30] Kaveh, A., Javadi, S. M., & Moghanni, R. M. (2020, December). Optimal structural control of tall buildings using tuned mass dampers via chaotic optimization algorithm. In *Structures* (Vol. 28, pp. 2704-2713). Elsevier.

[31] Lara-Valencia, L. A., Caicedo, D., & Valencia-Gonzalez, Y. (2021). A novel whale optimization algorithm for the design of tuned mass dampers under earthquake excitations. *Applied Sciences*, *11*(13), 6172.

[32] Kaveh, A., & Farhoudi, N. (2013). A new optimization method: Dolphin echolocation. *Advances in Engineering Software*, *59*, 53-70.

[33] Mirjalili, S., Mirjalili, S. M., & Lewis, A. (2014). Grey wolf optimizer. *Advances in engineering software*, *69*, 46-61.

[34] Mirjalili, S., & Lewis, A. (2016). The whale optimization algorithm. *Advances in engineering software*, *95*, 51-67.

[35] Daryan, A. S., Palizi, S., & Farhoudi, N. (2019). Optimization of plastic analysis of moment frames using modified dolphin echolocation algorithm. *Advances in Structural Engineering*, *22*(11), 2504-2516.

[36] Daryan, A. S., Salari, M., Farhoudi, N., & Palizi, S. (2021). Seismic design optimization of steel frames with steel shear wall system using modified Dolphin algorithm. *International Journal of Steel Structures*, *21*(3), 771-786.

[37] Palizi, S., & Daryan, A. S. (2020). Plastic analysis of braced frames by application of metaheuristic optimization algorithms. International Journal of Steel Structures, 20(4), 1135-1150.

[38] Toufigh, V., & Palizi, S. (2022). Performance evaluation of slag-based concrete at elevated temperatures by a novel machine learning approach. *Construction and Building Materials*, *358*, 129357.

[39] Mittal, N., Singh, U., & Sohi, B. S. (2016). Modified grey wolf optimizer for global engineering optimization. *Applied Computational Intelligence and Soft Computing*, *2016*.

[40] Daryan, A. S., Salari, M., Palizi, S., & Farhoudi, N. (2023, February). Size and layout optimum design of frames with steel plate shear walls by metaheuristic optimization algorithms. In *Structures* (Vol. 48, pp. 657-668). Elsevier.

[41] Li, Y., Han, M., & Guo, Q. (2020). Modified whale optimization algorithm based on tent chaotic mapping and its application in structural optimization. *KSCE Journal of Civil Engineering*, *24*(12), 3703-3713.

[42] Gandomi, A. H., & Yang, X. S. (2014). Chaotic bat algorithm. *Journal of Computational Science*, *5*(2), 224-232.

[43] Li, C., Li, S., & Lo, K. T. (2011). Breaking a modified substitution–diffusion image cipher based on chaotic standard and logistic maps. *Communications in Nonlinear Science and Numerical Simulation*, *16*(2), 837-843.

[44] Hadi, M. N., & Arfiadi, Y. (1998). Optimum design of absorber for MDOF structures. *Journal of Structural Engineering*, *124*(11), 1272-1280.

[45] Farshidianfar, A., & Soheili, S. (2013). Ant colony optimization of tuned mass dampers for earthquake oscillations of high-rise structures including soil–structure interaction. *Soil Dynamics and Earthquake Engineering*, *51*, 14-22.

[46] Mirzai, N. M., Zahrai, S. M., & Bozorgi, F. (2017). Proposing optimum parameters of TMDs using GSA and PSO algorithms for drift reduction and uniformity. *Struct Eng Mech*, *63*(2), 147-60.